



# Materiality Manipulation by Light-Field Projection from Reflectance Analysis

Kouki Murakami<sup>1</sup>  and Toshiyuki Amano<sup>1</sup> 

<sup>1</sup>Graduate School of Systems Engineering, Wakayama University, Japan

---

## Abstract

*In this paper, we report a method for changing the appearance of an object to different colors as a function of viewing perspective with multiple projectors and cameras. If such appearance manipulation becomes possible, morpho butterfly colors, metallic reflection, and other structural colors can be expressed. For such appearance editing, we proposed a reflection model which describes the optical response of projectors and cameras. We also propose methods for calculating the reflectance matrix and the optimized projection images using non-negative minimization. Through experimental results, we confirmed our method allowed perspective-dependent appearance to be designed by choosing the appropriate reflectance from the non-Lambert reflection area.*

## CCS Concepts

• **Human-centered computing** → Mixed / augmented reality; • **Computing methodologies** → Mixed / augmented reality;

---

## 1. Introduction

The angular distribution of scattered light from a surface involves surface reflection (e.g., BRDF; bidirectional reflectance distribution function, BTDF; bidirectional transmittance distribution function) and an illuminating light-field. Reflected light rays reach our retina, allowing us to perceive rich materiality such as glossy metallic reflections, nondirectional soft reflection from a plaster statue, and shiny reflections from a smooth plastic object, etc. It is remarkable that the angular distribution of scattered light can be manipulated by designing the illumination distribution, and this affects the object's appearance depending on perspective. Such appearance manipulation is one of the goals of the projection display technique, and this paper proposes materiality manipulation using light-field projection based on reflectance analysis in the context of spatial augmented reality (SAR).

SAR is widely known to non-experts as projection mapping. As pioneering work in SAR, Shader Lamps [RWLB01] allowed texture mapping with shadow animations on 3D building models. The virtual photometric environment system [MUK04] and the lighting environment enabled display of various reflection properties and their appearance through projection. Radiometric compensation is an advanced projection technique that projects the intended texture on a textured surface. Nayar et al. demonstrated such radiometric compensation by dynamic processing using a projector and camera [NPGB03].

Projection target is not limited to solid-color object, and it enables appearance-manipulation to textured surfaces. For example, projection display enables the virtual restoration of oil paintings

[YOS03] and of ancient clay vases [ALY08]. In addition, high-dynamic-range display [BI08] which combines object albedo and an overlay projection has been realized. Also, high-dynamic-range display techniques have been applied to improve the contrast of the object fabricated by a 3D printer [SIS11].

Appearance manipulation is another stream for projection display that enabled successive alternation of an object's appearance by feedback processing with a projector-camera system [AK10]. In addition, material appearance display [OOD10] and editing [LAS\*11] based on optical theory have been proposed. The manipulation capability is not limited to the object's color, but it also enabled manipulation of the materiality, such as transparency and glossiness [Ama13]. However, the aforementioned methods assume diffuse surface reflection occurs at the surface of the target object. Thus, it is impossible in principle to manipulate appearance such that it presents the correct directional reflected light distribution. Examples include structural color and metallic luster, where color changes with perspective.

To solve this problem, Amano et al. demonstrated appearance manipulation, which shows different manipulation depending on the perspective by using the multiple projector-camera feedback systems [AUM17]. However, because the system does not share the coordinates and images among projector-camera systems, manipulating the angular distribution of light on the target surface is impossible. Therefore, this study aims to demonstrate perspective-dependent appearance manipulation by modeling the reflection characteristics from objects and performing reflection analysis by using response models for multiple projectors and cameras

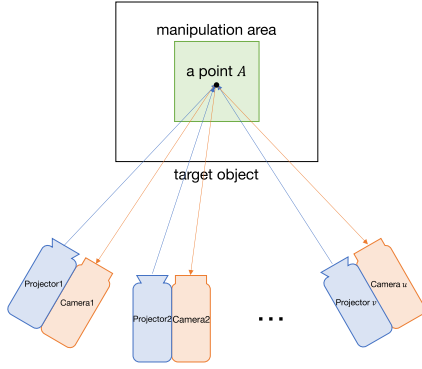


Figure 1: Conceptual diagram of method.

with a reflectance matrix. The main contribution of this paper is the formulation of direction-dependent appearance manipulation using light-field projection based on the analytical model for surface reflection.

## 2. Multiple Projector-Camera Response-model with Reflectance Matrix

In this study, we manipulated perspective-dependent material appearance using a projector array and a camera array (Figure 1). Each projector is arranged so that projection can be performed on the object from different directions, and each camera is arranged so as to be able to capture the object from different directions. In projection and capture with such devices, we define the RGB values at a point  $A$  in an image captured by camera  $i$  as

$$\hat{C}_i = (c_i^r, c_i^g, c_i^b)^T, c_i^r \geq 0, c_i^g \geq 0, c_i^b \geq 0, \text{ where } i = 1, 2, \dots, u. \quad (1)$$

Similarly, we define the RGB values at the point in a projection image corresponding to that point  $A$  from projector  $j$  as

$$\hat{P}_j = (p_j^r, p_j^g, p_j^b)^T, p_j^r \geq 0, p_j^g \geq 0, p_j^b \geq 0, \text{ where } j = 1, 2, \dots, v. \quad (2)$$

In this case, by expressing reflection at an object surface as a matrix  $\hat{K} \in \mathcal{R}^{3 \times 3}$ , it can be described as

$$\hat{C}_i = \hat{K}_{ij} M_{ij} \hat{P}_j, \quad (3)$$

where  $M_{ij}$  is the color mixing matrix [NPGB03] that calibrates the color. In this paper, we correct a difference in color due to individual differences by measuring  $M_{ij}$ .

Moreover, when multiple projectors and cameras are used, we propose

$$\tilde{C} = \tilde{K} \tilde{M} \tilde{P}, \quad (4)$$

where

$$\tilde{C} = (\hat{C}_1^T, \hat{C}_2^T, \dots, \hat{C}_u^T)^T, \tilde{P} = (\hat{P}_1^T, \hat{P}_2^T, \dots, \hat{P}_v^T)^T, \quad (5)$$

$$\tilde{M} = \begin{pmatrix} M_{11} & M_{12} & \dots & M_{1v} \\ M_{21} & M_{22} & \dots & M_{2v} \\ \vdots & \vdots & \ddots & \vdots \\ M_{u1} & M_{u2} & \dots & M_{uv} \end{pmatrix}, \tilde{K} = \begin{pmatrix} \hat{K}_{11} & \hat{K}_{12} & \dots & \hat{K}_{1v} \\ \hat{K}_{21} & \hat{K}_{22} & \dots & \hat{K}_{2v} \\ \vdots & \vdots & \ddots & \vdots \\ \hat{K}_{u1} & \hat{K}_{u2} & \dots & \hat{K}_{uv} \end{pmatrix}$$

Hereafter, we regard color spaces as calibrated and we write  $\tilde{M}\tilde{P}$  as  $\tilde{P}$  in the following sections.

## 3. Projection Images Calculation by a Non-Negative Minimization

Using the reflectance matrix and desired appearance  $\hat{C}_{t1}, \hat{C}_{t2}, \dots, \hat{C}_{tu}$ , we can obtain the projection images:

$$\tilde{P}_t = \tilde{K}^{-1} \tilde{C}_t, \quad (6)$$

where  $\tilde{C}_t = (\hat{C}_{t1}^T, \hat{C}_{t2}^T, \dots, \hat{C}_{tu}^T)^T, \tilde{P}_t = (\hat{P}_{t1}^T, \hat{P}_{t2}^T, \dots, \hat{P}_{tv}^T)^T$  that alters object appearance to desired appearances  $\hat{C}_{ti}$  for all perspectives by projection of  $\hat{P}_{tj}$  from projector  $j$ . However, data in projection images  $\hat{P}_{t1}^T, \hat{P}_{t2}^T, \dots, \hat{P}_{tv}^T$  should be positive, and equation (6) is not guaranteed to satisfy this condition. Therefore, we solve the non-negative least squares problem

$$\min_q \|\tilde{K} \tilde{P}_t - \tilde{C}_t\|_2, \text{ where } p_{t1}^r \geq 0, p_{t1}^g \geq 0, p_{t1}^b \geq 0, \dots, p_{tv}^b \geq 0. \quad (7)$$

using the Lawson–Hanson algorithm [LH74] to obtain non-negative optimized projection images.

## 4. Calibration of Multiple Projector-Camera Systems

Different projectors and cameras have different light or color sensitivities, even though we composed a system by identical model products. Since such individual differences leads to an imbalanced reflectance matrix estimation, we optically calibrated all projectors and cameras.

First, the light sensitivity of all cameras was adjusted, and we then unified the image brightness values among all cameras. For this adjustment, we employed a diffuse whiteboard as a reference and assumed that the observed brightness values from different viewing directions are identical. We then placed a whiteboard in front of the camera-array and adjusted each iris so that all cameras obtained an identical brightness. The exposure time and camera gain were set identical in all cameras.

Next, we performed color calibration. The white balance of the captured image can be changed by environmental illumination and faint power differences in the RGB projection gain in the projector. This will also produce imbalanced reflection matrices. Thus, color calibration was performed beforehand so that we observed same values in each channel when a white reference object was captured under environmental illumination.

For this calibration, we adjusted the gain in the RGB channels so that the RGB values observed at the whiteboard are identical. Then, we calculated the color-mixing matrix  $M_{ij}$  between the camera  $i$  and projector  $j$  for all possible combinations, thus obtaining  $\tilde{M}$ .

## 5. Experimental Setup

### 5.1. Multiple Projector-Camera Systems

If the system employed more projectors than cameras, the reflectance matrix can be estimated by using its generalized inverse. However, projection images for different angular light distributions



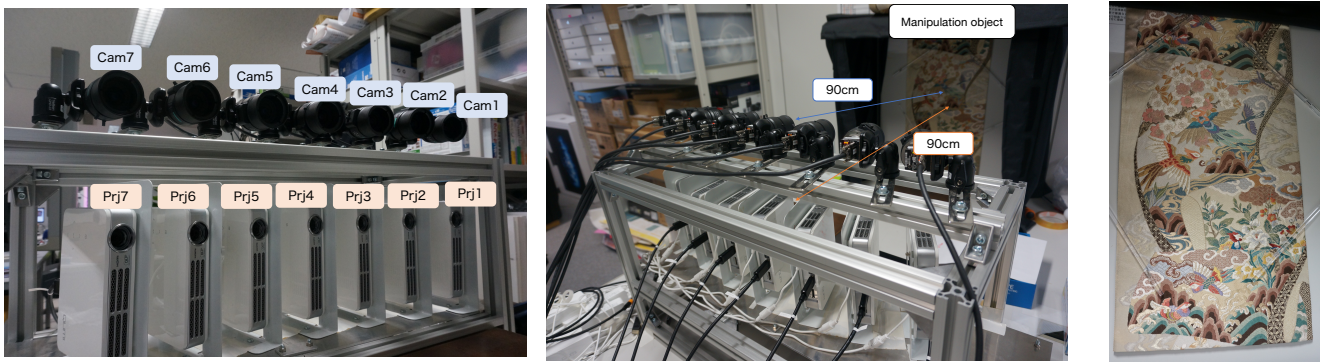


Figure 2: Experimental devices and the manipulation object.

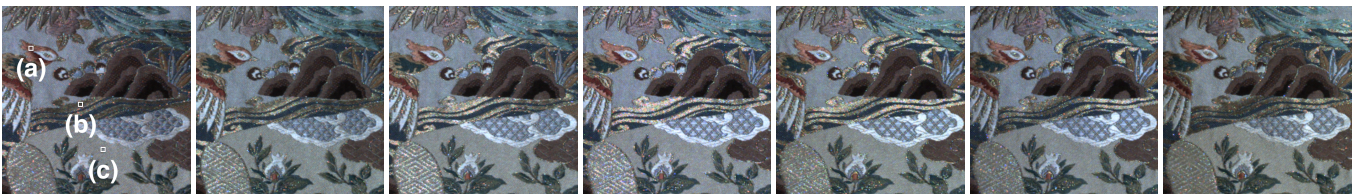


Figure 3: Object appearance when white projection was performed with  $Prj4$ . There is the brightness transition depending on perspective in the river crossing at the center of the object and the plumage in the left side of the object.

are not uniquely determined. Therefore, we equated the number of projectors with the number of cameras.

In this study, we employed 7 cameras (Ximea, MQ013CGE2) and 7 projectors (Vivitek, QUMIQ5-WT) in order to achieve high-quality perceptual BRDF manipulation with complex reflection characteristics. The cameras and projectors were placed in front of the target object and aligned on the horizontal plane to an azimuth angle of  $-15deg. \sim +15deg.$  in  $5deg.$  intervals to manipulate the material appearance. Therefore, we consider the horizontal only parallax for perceptual BRDF manipulation. Each camera was fixed at the same position as a corresponding projector in a dedicated frame using camera platforms (Figure 2). From left to right, we denote the cameras  $Cam1, Cam2, \dots, Cam7$ . In the same way, we denote the projectors  $Prj1, Prj2, \dots, Prj7$ .

The distance between a projector-camera array and the object is arranged to  $90cm$  so that all the projectors can project the same area and manipulate the appearance of the object, as shown at the middle of Figure 2.

## 5.2. Manipulation Target Object

We used a drawing foil of Nishijin silk textile, which contains patterns of birds, flowers, clouds, and a mountain with rivers, as the manipulation target. The drawing foil made with the sliced gold and silver leaves and silk strings is suited for our appearance manipulation technique due to its complex reflection and scattering characteristics. Figure 3 shows the appearance transition of the target object, which changes depending on perspective. The target object is illuminated by ordinary white environmental light, but the target object that has specular reflection caused by being woven from gold

thread. This changes the brightness in the river and plumage on the foil. Such anisotropic reflection characteristics enables manipulation of apparent color depending on perspective. In other words, the apparent BRDF changes which reflects changes in the material appearance depending on perspective. However, it is impossible to manipulate color depending on perspective in parts where purely diffuse reflection occurs. This is because purely diffuse reflection reflects incident light equally in all directions. Thus, even if multiple projections are incident from different positions onto the manipulation area, appearance changes cannot be seen from different perspectives. In this study, we regard the target object as a plane.

## 5.3. Acquisition of Reflectance Matrix

In this section, we explain in detail how we obtained the reflectance matrix  $\hat{K}$  with projectors and cameras.

First, we projected three color images of  $\hat{P}_j^r = (1, 0, 0)^T$ ,  $\hat{P}_j^g = (0, 1, 0)^T$ , and  $\hat{P}_j^b = (0, 0, 1)^T$  with projector  $j$ , and we captured the target object with each camera. This projection is performed by all projectors, and 21 color images were obtained, as shown in Figure 4. Assuming that  $\hat{D}_{ij}^r$  is the set of RGB values observed with camera  $i$  when projecting  $\hat{P}_j^r$ ,  $\hat{D}_{ij}^g$  is the set of RGB values observed with camera  $i$  when projecting  $\hat{P}_j^g$ , and  $\hat{D}_{ij}^b$  is the set of RGB values observed with camera  $i$  when projecting  $\hat{P}_j^b$ , we can define

$$(\hat{D}_{ij}^r \hat{D}_{ij}^g \hat{D}_{ij}^b) = \hat{K}_{ij} \begin{pmatrix} 1 & 0 & 0 \\ 0 & 1 & 0 \\ 0 & 0 & 1 \end{pmatrix}, \quad (8)$$

which follows from equation (3). Therefore, the reflectance matrix

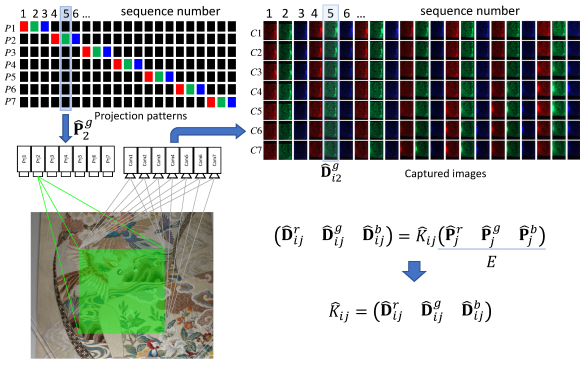


Figure 4: Acquisition of reflectance matrix.

$\hat{K}_{ij}$  that describes the response of camera  $i$  due to projector  $j$  can be calculated using

$$\hat{K}_{ij} = (\hat{D}_{ij}^r, \hat{D}_{ij}^g, \hat{D}_{ij}^b). \quad (9)$$

When we choose RGB values in the manipulation area from these captured images, points on the drawing foil do not correspond to the same coordinates in each image because each image was captured from a different perspective. Therefore, we performed a coordinate transformation in order to obtain the same object coordinates from different captured images. Specifically, we performed the coordinate transformation

$$S' = HS, \quad (10)$$

under the assumption of the planar shape of the target object. In this equation,  $H \in \mathcal{R}^{3 \times 3}$  is the projective transformation matrix calculated for each perspectives,  $S \in \mathcal{R}^3$  contains the homogeneous coordinates in the captured images before transformation, and  $S' \in \mathcal{R}^3$  contains the homogeneous coordinates in the captured images after transformation (Figure 5). We calculated this matrix  $H$  by referring to four points marked on the manipulation object.

In this study,  $\tilde{C}$  and  $\tilde{P}$  are  $3 \times 7 = 21$ -dimensional vectors, and  $\tilde{K}$  is a matrix with 21 rows and 21 columns because we used seven projectors and seven cameras. In order to determine the reflectance matrix  $\tilde{K}$ , it is necessary to project images with different colors from each projector more than three times, so we captured  $3 \times 7 = 21$  patterns with seven cameras; thus, we captured a total of 147 images. We attempted appearance manipulation by transformation of the captured images with the coordinate transformation (Equation 10) and we estimated the reflectance matrix using  $600 \times 600$  points within the manipulation area shown in Figure 5.

## 6. Apparent BRDF Manipulation Results

We projected the images calculated using equation 3 for each target onto the manipulation area of the object with each projector. Projection images were first generated in a common coordinate system ( $Cam4$ ) and then changed to the coordinate system for each projector using homography.

Figure 9 shows the manipulation results for color phase transition, contrast transition, and saturation transition as a function

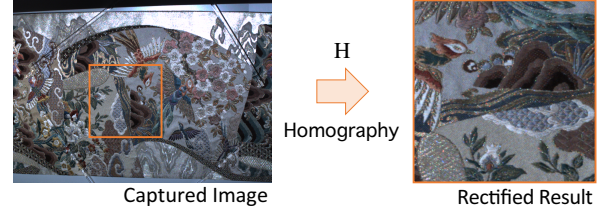


Figure 5: Homography transformation.

of apparent BRDF manipulation. In these results, the images captured by  $Cam1, Cam2, \dots, Cam7$  are shown from left to right, respectively.

### 6.1. Color Phase Transition

For the color phase transition, we set the first column in Figure 7 as the target images. We obtained these images by manipulating the hue values of the whole pixels with GNU Image Manipulation Program. This manipulation reference is centered on the perspective of  $Cam4$ , in which the hue in the manipulation area is decreased by  $40^\circ$  left and increased by  $40^\circ$  right. We solved the non-negative optimization problem explained in Section 3 and obtained the projection image in the first column in Figure 8.

These images show a strong tendency that the projected image from  $Prj7$  is reflected onto  $Cam1$  perspective due to its mirror reflection. Therefore, its tendency is remarkable in the area where specular reflection dominates. This reflection property is key of our apparent BRDF manipulation, and intended the color phase transition can be seen at the left bird area, central river area, and tail area in the upper right bird area in the first column of Figure 9.

Figure 6 shows the color phase transition along the viewing direction (horizontal axis). We calculated the average hue values of the  $5 \times 5$  pixels in three areas of target images and manipulation results. The point on the left bird (Figure 6 (a)) contains weak specular reflection. Also, the central river area pointed by (b) contains more strong specular reflection. Thanks to its property the color phase transition can be seen at these points. Contrary, because the diffuse reflection is dominant at the background area, it is difficult to achieve color phase transition on this area such as point (c).

### 6.2. Contrast Transition

The second column in Figure 7 shows the target images for the contrast transition. The contrast in the manipulation area increases toward the left and decreases toward the right. The second column in Figure 8 shows projection images for the contrast transition. The complementary color of the target object was projected to the river and the plumage areas that have specular reflection from  $Prj1$ . Conversely, the color of target object was projected from  $Prj7$ . Resultant images in the second column in Figure 9 show a contrast decrease from the perspective of  $Cam1$  toward the perspective of  $Cam7$ .

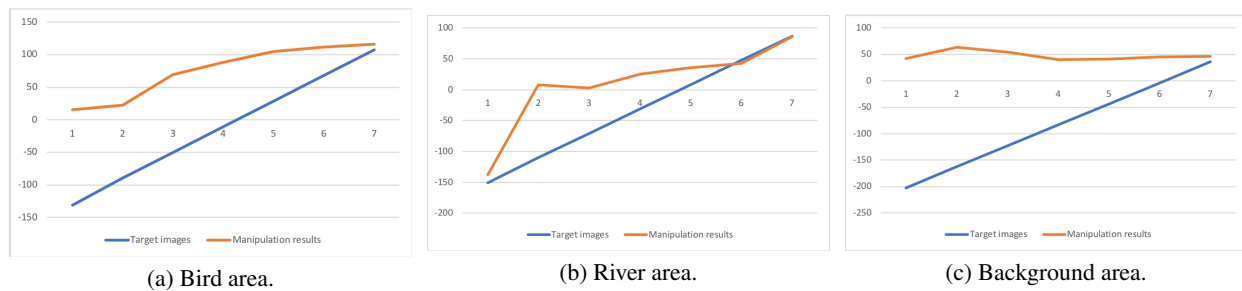


**Figure 6:** Color phase transition at some points by each viewing position (horizontal axis). (a) At the point of the left bird area. (b) At the point of the central river area. (c) At the point of the background area.

### 6.3. Saturation Transition

For the saturation transition, we set the target images shown in the last column in Figure 7. Contrary to contrast transition, the saturation in the manipulation area decreases toward the left and increases toward the right. The projection images for the saturation transition are shown in the last column in Figure 8. As with contrast transition, the color of target object was projected to areas that have specular reflection from  $Prj1$ . In the results shown in the last column in Figure 9, a saturation transition due to perspective changes can be confirmed in the left bird area, similar to the color phase transition. The intended saturation transition is observed in the area where specular reflection dominates.

## 7. Discussion

In Figure 9, perspective-dependent appearance changes cannot be observed in the background area of the object because color transitions according to perspective cannot be seen. This is because purely diffuse reflection dominates in this area. Since the diffusely reflected light is evenly reflected at all angles, reflected light from an object does not depend on perspective. Therefore, even though multiple projectors were used to project light on the object, reflected light from all the projectors is mixed and it is impossible to reproduce any perspective-dependent appearance transition. Thus, in order to demonstrate perspective-dependent appearance changes, there is a restriction that it is necessary to select an object with some level of specular reflection. The method proposed by Amano et al. [AUM17] assumes specular reflection at the surface of the object. In contrast, our method makes it possible to manipulate apparent BRDF since it is based on the reflectance matrix.

Figure 8 shows each manipulation is composed of three dominant images of  $Prj1$ ,  $Prj6$ , and  $Prj7$ . These images were calculated by the Lawson–Hanson algorithm [LH74] for its nonnegative constraint and it suggests that the reflection property of the textile has three degrees of freedom. In other words, the perspective-dependent appearance transition can be realized by only three projectors, but its angular resolution capability is restricted by its degrees of freedom.

## 8. Conclusion

An object's appearance can be manipulated by light field projection using multiple projectors by exploiting reflection of light from a complex surface.

In this study, we proposed a reflection model that describes the optical response of projectors and cameras, which illustrates a rough sample of BRDF. Moreover, we proposed an optical calibration method for multiple projectors and cameras. In addition, we described the methods used to calculate the reflectance matrix and the optimized projection images using non-negative minimization.

Using the obtained reflectance matrix and projection images, projection was used to manipulate the appearance of an object observed from different perspectives. The experimental results confirm that the perspective-dependent appearance was impossible in an area where diffuse reflection dominates. However, our method enabled perspective-dependent appearance manipulation to be designed based on the reflectance property from the non-Lambert reflection area.

## Acknowledgment

This work was supported by JSPS KAKENHI Grant Number 17H01781 and MEXT KAKENHI Grant Number 18H05008.

## References

- [AK10] AMANO T., KATO H.: Appearance control using projection with model predictive control. In *2010 20th International Conference on Pattern Recognition* (Aug 2010), pp. 2832–2835. doi:10.1109/ICPR.2010.694. 1
- [ALY08] ALIAGA D. G., LAW A. J., YEUNG Y. H.: A virtual restoration stage for real-world objects. *ACM Trans. Graph.* 27, 5 (Dec. 2008), 149:1–149:10. URL: <http://doi.acm.org/10.1145/1409060.1409102>, doi:10.1145/1409060.1409102. 1
- [Ama13] AMANO T.: Projection based real-time material appearance manipulation. In *2013 IEEE Conference on Computer Vision and Pattern Recognition Workshops* (June 2013), pp. 918–923. doi:10.1109/CVPRW.2013.135. 1
- [AUM17] AMANO T., USHIDA S., MIYABAYASHI Y.: Viewpoint-Dependent Appearance-Manipulation with Multiple Projector-Camera Systems. In *ICAT-EGVE 2017 - International Conference on Artificial Reality and Telexistence and Eurographics Symposium on Virtual Environments* (2017), Lindeman R. W., Bruder G., Iwai D., (Eds.), The Eurographics Association. doi:10.2312/egve.20171346. 1, 5





**Figure 7:** Target images. From the top to the bottom: color phase transition, contrast transition, saturation transition.

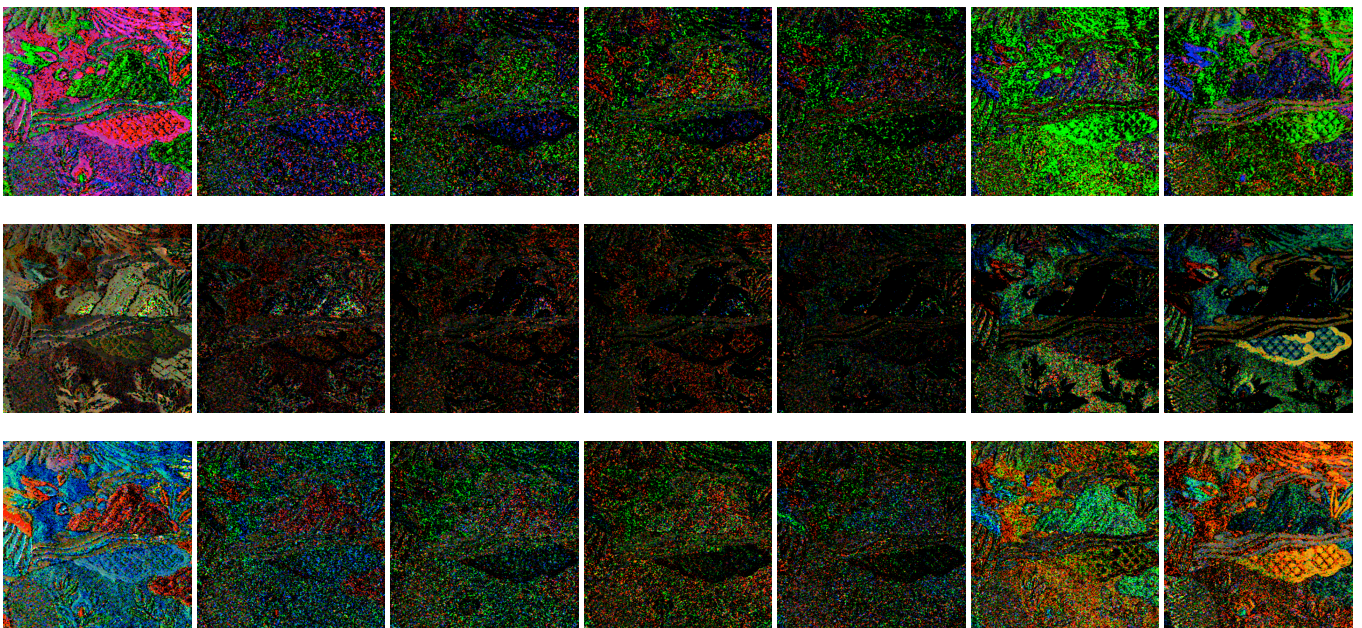


**Figure 8:** Projection images. From the top to the bottom: color phase transition, contrast transition, and saturation transition.

- [BI08] BIMBER O., IWAI D.: Superimposing dynamic range. *ACM Trans. Graph.* 27, 5 (Dec. 2008), 150:1–150:8. URL: <http://doi.acm.org/10.1145/1409060.1409103>, doi:10.1145/1409060.1409103. 1
- [LAS\*11] LAW A. J., ALIAGA D. G., SAJADI B., MAJUMDER A., PIZLO Z.: Perceptually based appearance modification for compliant appearance editing. *Computer Graphics Forum* 30, 8 (2011), 2288–2300. doi:10.1111/j.1467-8659.2011.02035.x. 1
- [LH74] LAWSON C. L., HANSON R. J.: *Solving least squares problems*.

Prentice Hall, 1974. 2, 5

- [MUK04] MUKAIGAWA Y.: Virtual photometric environment using projector. *Proc. International Conference on Virtual Systems and Multimedia (VSMM2004)* (2004). URL: <https://ci.nii.ac.jp/naid/10017297224/>. 1
- [NPG03] NAYAR S. K., PERI H., GROSSBERG M. D., BELHUMEUR P. N.: A projection system with radiometric compensation for screen imperfections. In *First IEEE International Workshop on Projector-Camera Systems (PROCAMS-2003)* (2003). 1, 2



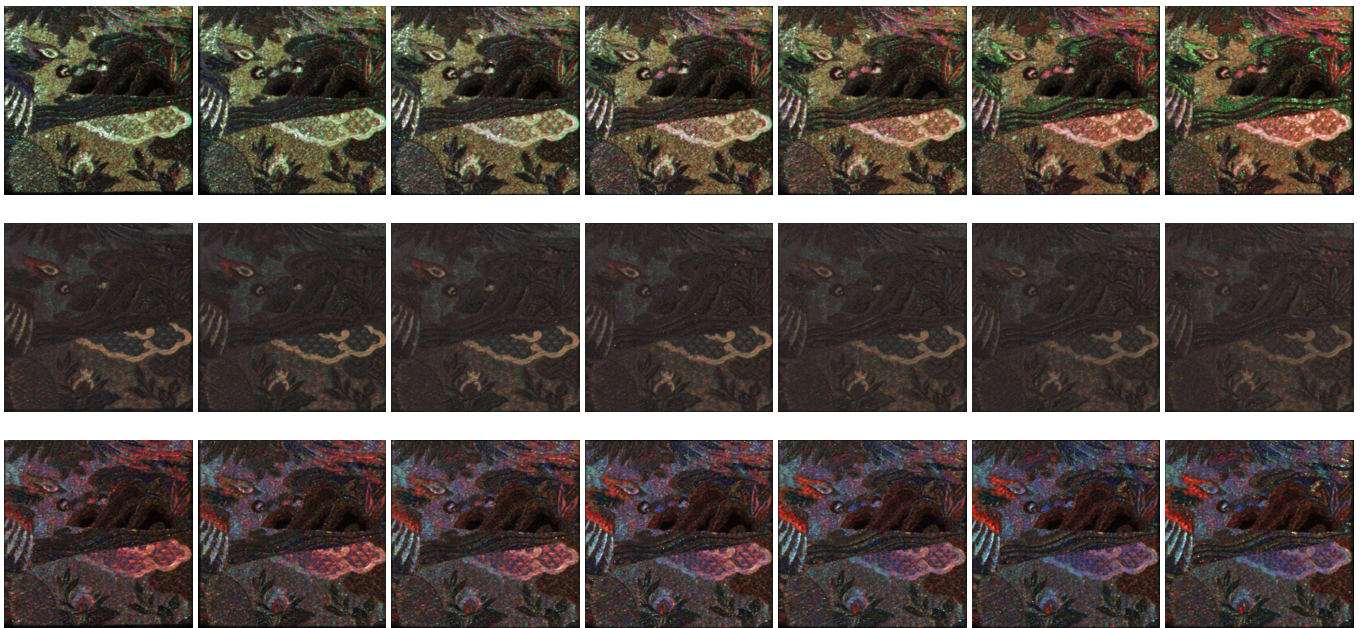


**Figure 9:** Material appearance edit results. From the top to the bottom: color phase transition, contrast transition, and saturation transition.

- [OOD10] OKAZAKI T., OKATANI T., DEGUCHI K.: A projector-camera system for high-quality synthesis of virtual reflectance on real object surfaces. *IPSI Transactions on Computer Vision and Applications* 2 (2010), 71–83. doi:10.2197/ipsjtcva.2.71. 1
- [RWLB01] RASKAR R., WELCH G., LOW K.-L., BANDYOPADHYAY D.: Shader lamps: Animating real objects with image-based illumination. In *Proceedings of the 12th Eurographics Workshop on Rendering Techniques* (London, UK, UK, 2001), Springer-Verlag, pp. 89–102. URL: <http://dl.acm.org/citation.cfm?id=647653.732300>. 1
- [SIS11] SHIMAZU S., IWAI D., SATO K.: 3d high dynamic range display system. In *2011 10th IEEE International Symposium on Mixed and Augmented Reality* (Oct 2011), pp. 235–236. doi:10.1109/ISMAR.2011.6092393. 1
- [YOS03] YOSHIDA T.: A virtual color reconstruction system for real heritage with light projection. *Proc. of VSMM, 2003* (2003), 1–7. URL: <https://ci.nii.ac.jp/naid/20001543329/>. 1